# Local delivery of antimicrobial peptides using self-organized TiO$_2$ nanotube arrays for peri-implant infections

Menghan Ma,[1] Mehdi Kazemzadeh-Narbat,[1] Yu Hui,[2] Shanshan Lu,[1] Chuanfan Ding,[3] David D. Y. Chen,[2] Robert E. W. Hancock,[4] Rizhi Wang[1]

[1]Department of Materials Engineering, University of British Columbia, Vancouver, BC, Canada
[2]Department of Chemistry, University of British Columbia, Vancouver, BC, Canada
[3]Department of Chemistry, Fudan University, Shanghai, People's Republic of China
[4]Department of Microbiology and Immunology, University of British Columbia, Vancouver, BC, Canada

**Abstract:** Peri-implant infections have been reported as one of the major complications that lead to the failure of orthopedic implants. An ideal solution to the peri-implant infection is to locally deliver antimicrobial agents through the implant surface. The rising problem of infections caused by multiple antibiotic-resistant bacteria makes traditional antibiotics less desirable for the prevention of peri-implant infections. One of the promising alternatives is the family of antimicrobial peptides (AMPs). In this study, we report the local delivery of AMPs through the nanotubular structure processed on titanium surface. Self-organized and vertically oriented TiO$_2$ nanotubes, about 80 nm in diameter and 7 $\mu$m thick, were prepared by the anodization technique. HHC-36 (KRWWKWWRR), one of the most potent broad-spectrum AMPs, was loaded onto the TiO$_2$ nanotubes via a simple vacuum-assisted physical adsorption method. Antimicrobial activity testing against Gram-positive bacterium, *Staphylococcus aureus*, demonstrated that this AMP-loaded nanotubular surface could effectively kill the bacteria (99.9% killing) and reduce the total bacterial number adhered to the surface after 4 h of culture. *In vitro* AMP elution from the nanotubes was investigated using liquid chromatography-mass spectrometry (LC-MS). The release profiles strongly depended on the crystallinity of the TiO$_2$ nanotubes. Anatase TiO$_2$ nanotubes released significantly higher amounts of AMP than amorphous nanotubes during the initial burst release stage. Both followed almost the same slow release profile from 4 h up to 7 days. Despite the differences in release kinetics, no significant difference was observed between these two groups in bactericidal efficiency. © 2011 Wiley Periodicals, Inc. J Biomed Mater Res Part A: 100A: 278–285, 2012.

**Key Words:** peri-implant infection, TiO$_2$ nanotubes, anodization, antimicrobial peptide, orthopaedic implants

---

**How to cite this article**: Ma M, Kazemzadeh-Narbat M, Hui Y, Lu S, Ding C, Chen DDY, Hancock REW, Wang R. 2012. Local delivery of antimicrobial peptides using self-organized TiO$_2$ nanotube arrays for peri-implant infections. J Biomed Mater Res Part A 2012:100A:278–285.

---

## INTRODUCTION

The successful application of orthopedic implants, including artificial joints and fracture fixation devices, has greatly improved the quality of life of many people suffering from aging related diseases, such as osteoarthritis and osteoporosis.[1–5] Among the various complications that lead to the failure of orthopedic implants, peri-implant infection has been reported as one of the major causes.[6,7] The overall infection rate associated with primary surgeries is estimated to be in the range of 0.5 to 5%, however, after revision surgery, the re-infection rate can significantly increase up to 14%.[5,8–10] The cost for treating such infections is estimated to be at least $50,000 per patient, while the associated mortality rate may be as high as 2.5%.[9,11,12] Despite the tremendous morbidity and economic burden, solutions to prevent peri-prosthetic infections have been very limited.

Peri-prosthetic infections are typically caused by microorganisms growing in structures, known as biofilms.[13,14] Despite strict sterilization and aseptic procedures, bacteria may still colonize on the implant surface at the time of surgery or at a later stage (e.g. via a hematogenous route).[15,16] Once growing into a biofilm on the implant surface, bacteria are 10 to 1000 times less susceptible to the host immune system and antibiotics mainly because of the poor antibiotic penetration into the biofilm and the stationary phase of growth of the bacteria underlying the surface layer.[5,17–19]

The most common pathogens causing peri-prosthetic infections are Gram-positive *Staphylococcus aureus* (20–25%, often the methicillin-resistant "Superbug" version, MRSA) and coagulase-negative staphylococci (20–30%, e.g. *Staphylococcus epidermis*).[5,9] To prevent or treat implant-related infections, antibiotics are used. However, both *S. aureus*

and *Staphylococcus epidermis* are known to have a high potential for developing resistance to traditional antibiotics, especially after the formation of biofilms on implant surfaces.[5] The development of antibiotic resistance can lead to devastating effects in the absence of an effective medical treatment to control the infection. One preferred solution for infection prevention is by using nontraditional antimicrobial agents such as cationic antimicrobial peptides (AMPs) that have a low possibility of developing resistance.[20] AMPs are widely distributed in living organisms, and function as part of their first line of defence.[20] In the past three decades, such AMPs have drawn significant attention because of their rapid bactericidal activity against a broad spectrum of bacteria and other microbes,[21–23] low toxicity and immunogenicity,[23] as well as complex killing mechanisms. Recently, significant progress has been made in the identification and synthesis of new AMPs by combining quantitative structure activity relationship (QSAR) modeling and rapid screening approaches by Hilpert et al., and a group of highly active small broad-spectrum AMPs have been reported.[24]

Local delivery of antimicrobial agents through implant surfaces is an ideal solution to the peri-implant infection problem with reference to the enhanced efficacy, lower probability for bacterial resistance, and the greater control over distribution of antibiotics to avoid systemic toxicity.[8,16,25,26] This strategy faces two key challenges. The first is the proper selection of the antimicrobials that can avoid antibiotic resistance. The second one is to develop a suitable drug loading system that can effectively deliver antibiotics on the surface of metallic orthopedic implants, without impairing peri-implant bone growth.

Titanium dioxide, or titania, is a promising orthopedic material with excellent biocompatibility. In the past decade, the fabrication of $TiO_2$ nanotubular structures by the anodization method has attracted wide interest because of their high surface-to-volume ratio, controllable dimensions, adjustable wettability, and simple processing procedures.[27–32] It has been reported that $TiO_2$ nanotube arrays on titanium surfaces can significantly accelerate osteoblast cell growth and adhesion *in vitro*[33] and improve bone formation and bonding strength *in vivo*.[34–36] In addition, since titania nanostructures are formed by the anodization of the titanium substrate itself, the coating has stronger mechanical adhesion than most bioceramic coatings (e.g. hydroxyapatite coating) processed by deposition techniques such as plasma spray, electrophoretic and electrolytic deposition.

In this study, we explored the possibility of using $TiO_2$ nanotubes as a carrier for AMP delivery. Despite active studies on using $TiO_2$ nanotubes to control the release of small molecules[37] and proteins,[38] there have been few reports on using nanotubes to deliver antibiotics, and none on AMPs. In this article, the antimicrobial activities and bacteria adhesion of AMP-loaded $TiO_2$ nanotubes surfaces were studied using the pathogenic Gram-positive bacterium, *S. aureus*. The *in vitro* AMP release profile from $TiO_2$ nanotubes and the effect of crystallinity (amorphous *vs.* anatase − crystalline) on the drug loading efficiency were also investigated using liquid chromatography-mass spectrometry (LC-MS).

## MATERIALS AND METHODS

### Fabrication and characterization of $TiO_2$ nanotubes

A typical 2-electrode system was used for the anodization process: commercially pure titanium foil (0.1 mm, 99.6% purity, Goodfellow) was used as the working electrode (anode), and a piece of platinum foil as the cathode. Before anodizing, Ti foils were cleaned ultrasonically in acetone, absolute ethanol, and distilled water for 15 min sequentially, and air-dried. The anodization process was carried out in 98% ethylene glycol ($C_2H_6O_2$, Fisher Scientific, Canada) solution containing $0.27M$ ammonium fluoride ($NH_4F$, Fisher Scientific, Canada) at 30 V for 6 h, following the protocol of Macak et al.[39] with modified parameters. After the experiments, the samples were rinsed with distilled water three times for 30 s each, and then cleaned ultrasonically in absolute ethanol for 5 min.

To investigate the effect of annealing on the morphology and crystal structure of the $TiO_2$ nanotube coatings, as well as the influence of crystallinity on the AMP drug loading and antimicrobial efficacy, the processed nanotubes were annealed before peptide loading. The annealing was carried out in a chamber furnace (CARBOLITE Type 3216). Specimens were heated from room temperature to 400°C in air at the rate of 5°C/min, held for 3 h, and cooled down in the furnace.

The crystal phases of the nanotube coatings were examined using a Renishaw InVia Confocal Raman Microscope equipped with HeNe and Ar lasers. Field emission scanning electron microscopy (FESEM Hitachi S-4700) was used for morphological analysis of the titanium oxide coatings, and the thickness of the coatings was measured directly from the SEM cross-sectional images of mechanically bent samples.

### Antimicrobial peptide loading onto $TiO_2$ nanotube

HHC-36 (KRWWKWWRR), one of the most potent broad-spectrum AMPs identified in a recent large quantitative structure-activity relationship (QSAR) study[23] was chosen as the test AMP in this study. The peptide was purchased from CPC Scientific (Sunnyvale, CA) and demonstrated by HPLC and mass spectrometry to be >95% pure. To load HHC-36 into the nanotube samples, a 2 mg/mL peptide solution was prepared by dissolving HHC-36 powder into a phosphate buffer solution (50 m$M$ $Na_2HPO_4$, and the pH value was adjusted by $0.1N$ NaOH to 7.40). Samples (1 × 1 cm) were immersed into 1 mL of this peptide solution in glass vials, and the vials were placed in a vacuum desiccator for 30 min and then kept for 20 h at 23°C under constant, gentle shaking. After that, the samples were rinsed three times with the same buffer solution for 30 s each, to remove the excess peptide on the surface.

### *In vitro* release of AMP

The *in vitro* drug release profile of the AMP-loaded nanotube samples (both as-prepared nanotubes and 400°C annealed nanotubes) were studied using LC-MS. The samples were immersed in 1 mL distilled water in a capped vial and kept shaking at 37°C (Orbital Incubator Shaker,

Gyromax 737). The release medium was exchanged at regular intervals for up to 7 days (i.e. 1, 4, 24, 72, 168 h). After day 7, samples were dried and kept for further analysis. A series of standard solutions with known concentration of HHC-36 were tested together with the AMP-loaded nanotube samples to provide a calibration curve by which the AMP concentration could be calculated (External Standard Method).

The LC-MS quantifications were performed on Varian 210 Prostar solvent delivery system coupled with 1200L triple quadruple mass spectrometer. Kinetex 100 $\times$ 2.10 mm XB-C18 column packed with 2.6 $\mu$m core-shell particles was used for liquid chromatography. A gradient elution chromatography program comprised of three linear components: from 0 to 10 min, 2 to 20%B; from 10 to 12 min 20% B; from 12 to 15 min, 2% B, with 0.1% formic acid in water as mobile phase A, 0.1% formic acid in acetonitrile as mobile phase B, and flow rate at 0.2 mL/min. Mass spectrometry conditions tuned to give optimal sensitivity were: needle voltage at 3000 V, drying gas at 300°C and 21 psi, capillary voltage at 40 V, shield voltage at 400 V, and detector at 1700 V. $O$-methyl-tyrosine ($m/z$ 196.0) as internal standard and AMP ($m/z$ 299.0, 373.0, 497.0) as analyte were monitored through multiple ion channels.

### Antimicrobial test against S. aureus

Antimicrobial activities of the specimens were tested against the Gram-positive bacterium, $S.$ $aureus$ ATCC 25293. Before the test, the bacteria were grown overnight at 37°C in Mueller Hinton Broth (MHB). After that, 100 $\mu$L of the original bacterial solution was transferred into a sterile tube containing 5 mL MHB and incubated for 1 h at 37°C to obtain bacteria in the mid logarithmic phase of growth. The $S.$ $aureus$ bacterial suspension was then resuspended in MHB to dilute the solution and provide a final density of $\sim$106 bacteria/mL.

To test the bacterial killing ability of the AMP-loaded samples, a survival assay was performed. Five groups of samples (three specimens in each group) were investigated: negative control (bacteria solution), as-prepared $TiO_2$ nanotubes (ApNT), as-prepared $TiO_2$ nanotubes loaded with AMP (ApNT-AMP), 400°C annealed $TiO_2$ nanotubes (AnNT), and 400°C annealed $TiO_2$ nanotubes loaded with AMP (AnNT-AMP). The samples were first placed in a 12-well culture dish, and 1 mL of bacterial solution (density $\sim$10$^6$ bacteria/mL) was dripped into each well. After 1 h and 4 h incubation with the bacteria suspension (37°C, humidified, 5% $CO_2$ and 20% $O_2$, orbital shaking at 70 rpm), the residual bacteria were plated on nutrient agar and incubated overnight at 37°C, and the surviving bacteria were analyzed by assessing colony forming units (CFU).

### Bacterial adhesion on sample surfaces

Bacterial adhesion and the morphologies of the $S.$ $aureus$ colonies formed on different sample surfaces were studied using scanning electron microscopy (SEM; Hitachi S3000N). The samples from the antimicrobial test, after 4 h of bacterial growth, were examined using SEM. Before imaging, samples were first rinsed three times with 0.1$M$ phosphate buffered saline (PBS) and then fixed in 2.5% glutaraldehyde in 0.1$M$ PBS for 2 h at room temperature. After that, the samples were rinsed three times with 0.1$M$ PBS and dehydrated in graded ethanol (50, 70, 80, 90, 95, and 100%) for 15 min each. Finally, the samples were dried in $CO_2$ critical point dryer (Autosamdri®-815B, Series A) and gold sputtered using Denton Vacuum Desk II sputtering machine (Moorestown, NJ). The total bacteria number (live and dead) was counted on the SEM images. Five images for each sample without peptide and 20 images for each peptide-loaded sample (because of the high standard deviation) were taken at random locations on all the three samples in each group.

### Statistical analyses

The differences between all values were analyzed with the Holm $t$-test. The confidence level was set at 0.05 ([$alpha$] = 0.05), whereby a $p$ value lower than 0.05 indicated a statistically significant difference between testing groups.

## RESULTS

### Morphology of TiO$_2$ nanotubes

Figure 1 shows the SEM micrographs of the $TiO_2$ nanotubular structure. $TiO_2$ nanotubes were about 80 nm in diameter and 7 $\mu$m thick; oriented vertically to the sample surface. The nanotubes were highly ordered, hexagonal close packed [each nanotube was surrounded by six nearest neighbors, Fig. 1(a)] and uniformly distributed over the titanium surface. Ripples were observed on the side wall of the tubes [Fig. 1(b)]. Those ripples were the thickness fluctuations along the nanotubes,[40,41] and could be attributed to the periodic oscillations of the current during anodization.[40,27]

After annealing, the nanotubular morphology of the samples did not change. Raman Spectroscopy was performed over the range of 200 to 700 cm$^{-1}$, an optimal range for discriminating between different crystal phases of $TiO_2$.[42] Due to its metallic nature, Ti substrate does not have any peaks in the Raman spectrum.[43] As shown in Figure 2, the as-prepared nanotube sample did not have any obvious peaks within this range, indicating its amorphous nature. On the other hand, 400°C annealed sample showed typical anatase peaks at ˜400 cm$^{-1}$ (B1g vibration mode), ˜520 cm$^{-1}$ (A1g mode), and ˜640 cm$^{-1}$ (Eg mode)[42,43] which suggested a phase transformation of $TiO_2$ nanotubes from the amorphous to the anatase phase during annealing.

### In vitro release of AMP

The $in$ $vitro$ AMP release profiles from $TiO_2$ nanotubes (as-prepared $vs.$ 400°C annealed) were tested by LC-MS for up to 7 days. For both groups, high release rate was observed in the first 4 h, followed by a steady and relatively slow drug release (shown in Fig. 3). Although significantly higher AMP release was detected for anatase $TiO_2$ nanotubes than the amorphous samples during the initial burst release stage, both followed almost the same slow release profile from 4 h to 7 days. After 7 days of release, the
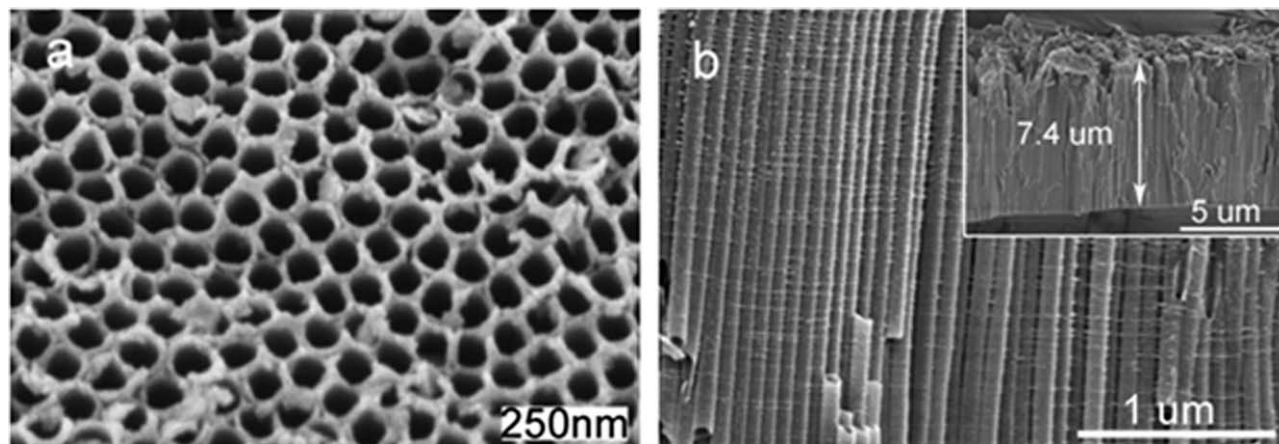
**FIGURE 1.** SEM micrographs of TiO$_2$ nanotubes. (a) Top view, (b) cross-sectional view. Anodized in 98% ethylene glycol solution containing 0.27$M$ NH$_4$F at 30 V for 6 h.

samples were examined with SEM and the nanotubes coatings were found to remain intact on the Ti surface.

### Antimicrobial activity

The antimicrobial activity of different surfaces against *S. aureus* is shown in Figure 4. Four groups of specimens were investigated: as-prepared TiO$_2$ nanotubes (ApNT), as-prepared TiO$_2$ nanotubes loaded with AMP (ApNT-AMP), annealed TiO$_2$ nanotubes (AnNT), annealed TiO$_2$ nanotubes loaded with AMP (AnNT-AMP), and the same *S. aureus* bacteria solution as the control group. Both ApNT and AnNT group showed similar bacterial growth to the control group ($p > 0.05$) with the bacterial colony forming units (CFU) increasing by about 100-fold in 4 h. Therefore, TiO$_2$ nanotubes without AMP did not have any antimicrobial activity. On the other hand, both ApNT-AMP and AnNT-AMP group demonstrated progressive and potent bacterial killing with an approximately 99.9% decrease (~1000-fold decrease compared with the initial input dose and 10$^5$-fold relative

to controls) in bacterial CFU (representing residual viable bacteria) observed after 4 h of incubation. No statistically significant difference was found between the two peptide loaded nanotubes surfaces ($p = 0.837$ for 1 h and $p = 1$ for 4 h). The results suggest that the AMPs loaded onto the TiO$_2$ nanotubes, as-prepared or annealed, can elute from the nanotubes continuously and effectively kill the bacteria in the surrounding environment of the implants.

### Bacteria adhesion on sample surfaces

The *S. aureus* bacterial colonies on the tested sample surfaces did not vary in their SEM morphology (Fig. 5). However, there were obviously more bacteria colonies on the samples without peptide (ApNT and AnNT) than the peptide-loaded samples (ApNT-AMP and AnNT-AMP). Figure 6 shows the total bacteria colony (live and dead) number counted from
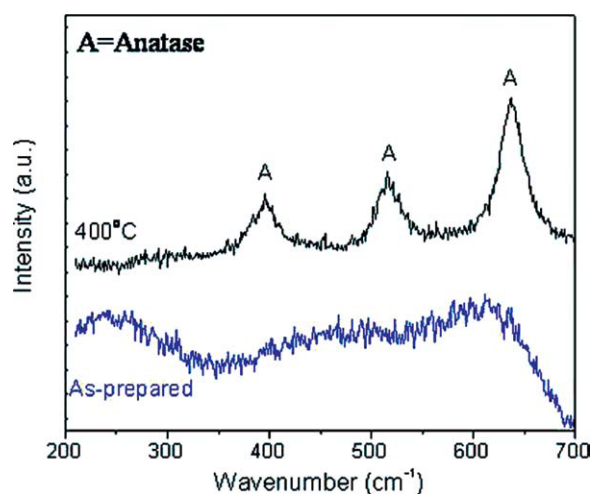


**FIGURE 2.** Raman spectra of TiO$_2$ nanotubes: as-prepared and 400°C annealed. [Color figure can be viewed in the online issue, which is available at wileyonlinelibrary.com.]
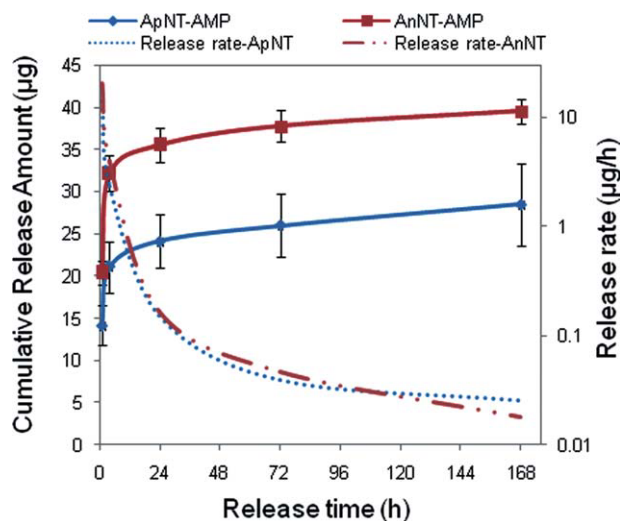


**FIGURE 3.** *In vitro* release of AMP from TiO$_2$ nanotube-coated Ti. Error bars indicate standard deviation ($n = 4$). ApNT-AMP: as-prepared TiO$_2$ nanotubes loaded with AMP; AnNT-AMP: annealed TiO$_2$ nanotubes loaded with AMP. [Color figure can be viewed in the online issue, which is available at wileyonlinelibrary.com.]
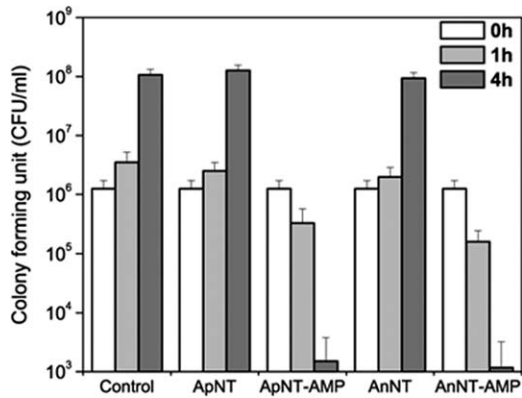
**FIGURE 4.** Antimicrobial activity against *S. aureus.* Residual colony counts after 1 and 4 h of incubation with different surfaces are shown. Control: bacteria solution. ApNT: as-prepared $TiO_2$ nanotubes; ApNT-AMP: as-prepared $TiO_2$ nanotubes loaded with AMP; AnNT: annealed $TiO_2$ nanotubes; AnNT-AMP: annealed $TiO_2$ nanotubes loaded with AMP.



**FIGURE 6.** Total *S. aureus* bacterial number after 4 h culture on different sample surfaces. Error bars indicate standard deviation ($n = 3$). ApNT: as-prepared $TiO_2$ nanotubes; ApNT-AMP: as-prepared $TiO_2$ nanotubes loaded with AMP; AnNT: annealed $TiO_2$ nanotubes; AnNT-AMP: annealed $TiO_2$ nanotubes loaded with AMP. [Color figure can be viewed in the online issue, which is available at wileyonlinelibrary.com.]

the SEM images. About 200-fold decrease was observed for the peptide-loaded groups compared with the groups without peptide. This result further supports the CFU results in Figure 4 and can be explained by the elution of AMP from the AMP-loaded samples, and subsequent bactericidal activity.

## DISCUSSION

In this study, we demonstrated that AMP (HHC-36) can be successfully loaded onto the $TiO_2$ nanotubes via the vacuum-assisted physical adsorption method. The antimicrobial test against *S. aureus* showed that these novel peptide-loaded nanotube surfaces (both amorphous and anatase phases) killed bacteria continuously and effectively reduced bacterial adhesion onto the surfaces. *In vitro* AMP elution tests suggested that the AMP was released slowly for up to 7 days after an initial burst of release. Using AMP-loaded $TiO_2$ nanotubes as a coating for orthopedic implants might be a potential solution for preventing periprosthetic infections.
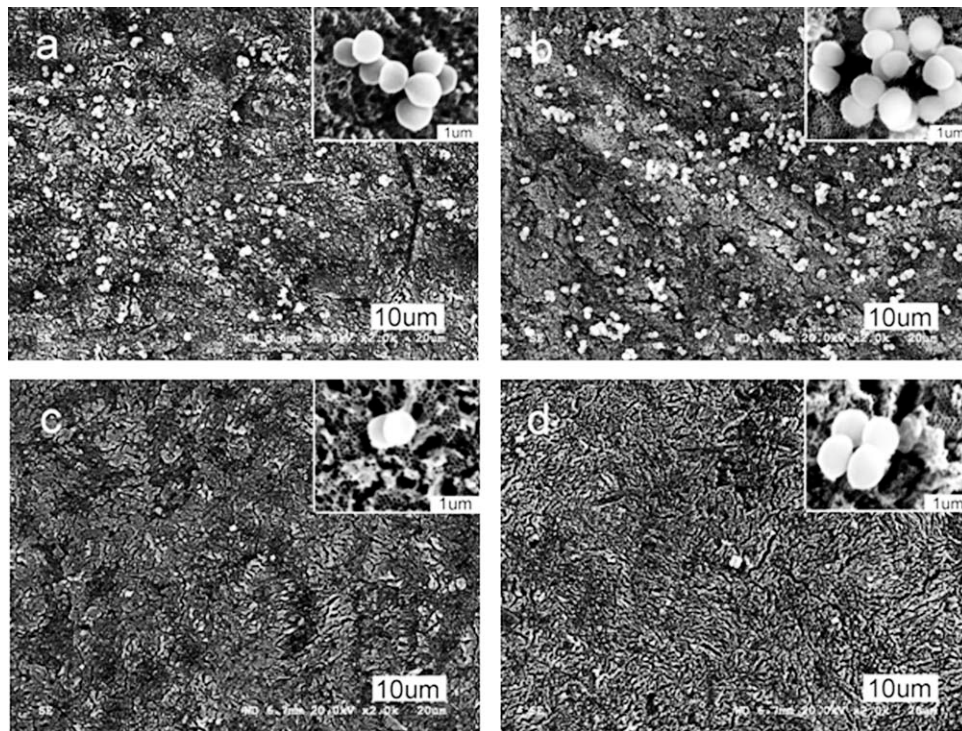


**FIGURE 5.** SEM images of *S.aureus* colonies after 4 h culture on: (a) ApNT: as-prepared $TiO_2$ nanotubes; (b) AnNT: annealed $TiO_2$ nanotubes; (c) ApNT-AMP: as-prepared $TiO_2$ nanotubes loaded with AMP; (d) AnNT-AMP: annealed $TiO_2$ nanotubes loaded with AMP, respectively.

ANTIMICROBIAL PEPTIDES ON NANOTUBES FOR PERI-IMPLANT INFECTIONS

The rising problem of infections caused by multiantibiotic-resistant bacteria, such as methicillin-resistant *S. aureus* (MRSA), makes traditional antibiotics a nonideal solution for peri-implant infections. Therefore, in this study, cationic AMPs were selected as an alternative to traditional antibiotics because of their rapid bactericidal activity against a broad spectrum of bactericial strains, low toxicity, as well as the complex killing mechanisms that reduce the development of resistance. AMPs have complex mechanisms of antimicrobial activity. Previous studies suggested that AMPs may interact with bacterial surfaces to either permeabilize them or to translocate across the cytoplasmic membrane to attack cytoplasmic targets.[44] In most cases more than one killing mechanism can be observed with a single peptide. As a result of their complex killing mechanisms, the possibility of developing a resistant mutant is significantly reduced.

The AMP selected in this study, HHC-36 (KRWWKWWRR), is one of the most potent peptides identified through high-throughput peptide screening (peptide arrays on cellulose and rapid screening technologies) in combination with quantitative structure activity relationship (QSAR) modeling. *In vitro* tests demonstrated that this peptide has better antimicrobial activities against a broad array of multidrug-resistant "Superbugs," including MRSA, than some highly used traditional antibiotics and the most advanced clinical candidate antimicrobial peptide (MX-226).[23] Moreover, it showed very low toxicity in metabolically active cells and caused minimal red blood cell lysis for concentrations up to 251 $\mu M$.[23]

$TiO_2$ nanotubes prepared by the anodization method have high surface-to-volume ratio, controllable diameter and length, and excellent biocompatibility.[29,45,46] They are therefore considered as an ideal drug delivery carrier. Previous studies have shown promising results. For example Popat et al.[38] demonstrated the controllable release of proteins (bovine serum albumin and lysozyme), loaded onto $TiO_2$ nanotubes (80 nm diameter and 400 nm long), in the order of hours. Peng et al.[37] reported the influence of $TiO_2$ nanotube size (diameter/length) on the drug loading amount and release profile, and illustrated the possibility of controlling long-term elution of small molecule and protein. Despite the promising capability of the nanotubes, there have been very few reports on using nanotubes to deliver antibiotics. Popat et al.[26] successfully loaded gentamicin into $TiO_2$ nanotubes. But their tests (against *Staphylococcus epidermis*) showed a relatively limited inhibition rate, only approximately 70% inhibition after 4 h of culture. In this study using the antimicrobial peptide (HHC-36), we achieved a much higher bacteria killing efficiency (99.9% bacteria killing after 4 h of culture). The results may be attributed to the rapid and enhanced bactericidal ability of the AMP used. As far as we know, this is the first report on AMP delivery using $TiO_2$ nanotubes. Titania nanotubes have certain advantages over other delivery coatings such as the calcium phosphate coating we reported recently.[19] Although with calcium phosphate coatings a fast bactericidal effect was observed within 30 min, the electrolytically processed calcium phosphate coating has less capability to control

drug release and suffers from a weak coating/substrate interface.

Peri-implant infections are the result of bacterial adhesion and subsequent biofilm formation at the implantation site.[47] The adhesion of bacteria onto implanted biomaterial surfaces is a critical step for pathogenesis of implant-related infections. After surgery, the bacteria that cannot attach quickly onto the implant surface will be rapidly killed by the immune system.[26] Our bacterial adhesion study showed that AMP-loaded nanotube samples effectively reduced bacterial number attached on the surfaces after 4 h of culture. This reduction may have come from the combined effect of the possible prevention of the original adhesion and the subsequent growth inhibition or killing of the bacteria. It is thus expected that using such AMP-loaded $TiO_2$ nanotube coatings for orthopedic implants can effectively protect the surface from the colonization by microbes, which would lead to a lower possibility of peri-implant infections.

Ideal local antibiotic release profiles for implant-related infection should exhibit burst release (high release rate) in the initial stage to rapidly kill all bacteria attached to the implant during the surgery, followed by a long-term drug release with a therapeutically effective dosage to continually prevent infection.[48] In this study, the *in vitro* elution kinetics test (Fig. 3) showed a burst release in the first 4 h, and a consistent and slow release of AMP up to 7 days. This result also indicated a relatively strong interaction between the tested peptide (HHC-36) and $TiO_2$ nanotubes. It has been reported in literature that various proteins and biomolecules can attach onto $TiO_2$ surfaces via physical adsorption methods.[49–52] The mechanism for physical adsorption on titanium dioxide surface is generally interpreted as a combination of electrostatic and Van der Waals forces.[49,51] HHC-36 has an isoelectric point of 12.7 (pI = 12.7) with five positively charged residues (Arg and Lys), which makes it highly positively charged at physiological pH (7.4, also the pH value of the buffer solution we used for drug loading). On the other hand, the isoelectric point of $TiO_2$ nanotubes is about 5.3;[53,54] thus, $TiO_2$ surface has a net negative charge at the working pH (7.4). Therefore, a strong electrostatic interaction between $TiO_2$ nanotubes and AMP molecules is expected, leading to the effective drug loading. Furthermore, $TiO_2$ nanotube coating is highly polar and superhydrophilic, which makes it easier for water to penetrate into the nanotubes.

An interesting result is the effect of $TiO_2$ crystallinity on the drug loading efficacy. Although no significant difference was observed between the amorphous and anatase group (ApNT-AMP and AnNT-AMP) in terms of bacterial killing rate against *S. aureus* (Fig. 4), higher amount of AMP was detected in the anatase phase $TiO_2$ nanotube samples. To understand the AMP loading behavior on $TiO_2$ nanotubes in the buffer solution (pH = 7.4) used for the AMP loading process, the zeta potentials of the $TiO_2$ nanotubes (both as-prepared and 400°C annealed) were measured. $TiO_2$ nanotubes were peeled off from the Ti surface and dispersed ultrasonically for 30 min in the buffer solution, and the zeta potentials were measured using a zeta meter (ZETA-METER system 3.0+). Higher

zeta potential was observed for anatase $TiO_2$ nanotubes ($-33.5$ mV) than the amorphous ones ($-29$ mV), which might be the reason for the higher AMP loading in the anatase phase (Fig. 3). Interestingly, previous studies have shown that the anatase phase $TiO_2$ is more favorable than the amorphous phase for bone growth possibly due to better lattice match with hydroxyapatite, the mineral component similar to that of natural bone tissue.[33,55,56] Also, Yu et al.[57] illustrated that anatase phase $TiO_2$ nanotubes have better corrosion resistance than the amorphous phase in naturally aerated Hank's solution. Combining our drug release and antimicrobial results with those reports, we could conclude that anatase phase is a better candidate than the as-prepared amorphous state for orthopedic applications.

## CONCLUSION

Self-organized, vertically oriented titanium dioxide nanotubes were successfully fabricated using the anodization method. A potent AMPs, HHC-36, was loaded into this tubular structure by a simple vacuum-assisted physical adsorption method. Anatase nanotubes showed better AMP loading efficiency than the amorphous phase. This AMP-loaded nanotubular surface could significantly kill *S. aureus* bacteria and effectively reduce bacterial adhesion on the surface.

## ACKNOWLEDGMENTS

## REFERENCES

1. Mariani BD, Tuan RS. Advances in the diagnosis of infection in prosthetic joint implants. Mol Med Today 1998;4:207–213.
2. Bozic KJ, Kurtz SM, Lau E, Ong K, Vail TP, Berry DJ. The epidemiology of revision total hip arthroplasty in the United States. J Bone Joint Surg Am 2009;91:128–133.
3. Goldhahn J, Suhm N, Goldhahn S, Blauth M, Hanson B. Influence of osteoporosis on fracture fixation—A systematic literature review. Osteoporosis Int 2008;19:761–772.
4. Canadian Institute for Health Information, Hip and Knee Replacements in Canada—Canadian Joint Replacement Registry (CJRR) 2008–2009 Annual Report (Ottawa, Ontario: CIHI, 2009).
5. Campoccia D, Montanaro L, Arciola CR. The significance of infection related to orthopedic devices and issues of antibiotic resistance. Biomaterials 2006;27:2331–2339.
6. Antoci V, Jr, Adams CS, Parvizi J, Davidson HM, Composto RJ, Freeman TA, Wickstrom E, Ducheyne P, Jungkind D, Shapiro IM, Hickok NJ. The inhibition of *Staphylococcus epidermidis* biofilm formation by vancomycin-modified titanium alloy and implications for the treatment of periprosthetic infection. Biomaterials 2008;29:4684–4690.
7. Antoci V, Jr, King SB, Jose B, Parvizi J, Zeiger AR, Wickstrom E, Freeman TA, Composto RJ, Ducheyne P, Shapiro IM, Hickok NJ, Adams CS. Vancomycin covalently bonded to titanium alloy prevents bacterial colonization. J Orthop Res 2007;25:858–866.
8. Zilberman M, Elsner JJ. Antibiotic-eluting medical devices for various applications. J Control Release 2008;130:202–215.
9. Sia IG, Berbari EF, Karchmer AW. Prosthetic joint infections. Infect Dis Clin North Am 2005;19:885–914.
10. Ewald A, Glueckermann SK, Thull R, Gbureck U. Antimicrobial titanium/silver PVD coatings on titanium. Biomed Eng Online 2006;5:22.
11. Sculco TP. The economic-impact of infected joint arthroplasty. Orthopedics 1995;18:871–873.
12. Lentino JR. Prosthetic joint infections: Bane of orthopedists, challenge for infectious disease specialists. Clin Infect Dis 2003;36:1157–1161.
13. Trampuz A, Osmon DR, Hanssen AD, Steckelberg JM, Patel R. Molecular and antibiofilm approaches to prosthetic joint infection. Clin Orthop Relat Res 2003:69–88.
14. Trampuz A, Zimmerli W. Prosthetic joint infections: Update in diagnosis and treatment. Swiss Med Wkly 2005;135:243–251.
15. Schmalzried TP, Amstutz HC, Au MK, Dorey FJ. Etiology of deep sepsis in total hip-arthroplasty—The significance of hematogenous and recurrent infections. Clin Orthop Relat Res 1992:200–207.
16. Zhao L, Chu PK, Zhang Y, Wu Z. Antibacterial coatings on titanium implants. J Biomed Mater Res B Appl Biomater 2009;91:470–480.
17. Darouiche RO. Current concepts—Treatment of infections associated with surgical implants. N Engl J Med 2004;350:1422–1429.
18. Costerton JW, Stewart PS, Greenberg EP. Bacterial biofilms: A common cause of persistent infections. Science 1999;284:1318–1322.
19. Kazemzadeh-Narbat M, Kindrachuk J, Duan K, Jenssen H, Hancock REW, Wang R. Antimicrobial peptides on calcium phosphate-coated titanium for the prevention of implant-associated infections. Biomaterials 2010;31:9519–9526.
20. Jenssen H, Hamill P, Hancock REW. Peptide antimicrobial agents. Clin Microbiol Rev 2006;19:491–511.
21. Mookherjee N, Hancock REW. Cationic host defence peptides: Innate immune regulatory peptides as a novel approach for treating infections. Cell Mol Life Sci 2007;64:922–933.
22. Hilpert K, Elliott MR, Volkmer-Engert R, Henklein P, Donini O, Zhou Q, Winkler DF, Hancock RE. Sequence requirements and an optimization strategy for short antimicrobial peptides. Chem Biol 2006;13:1101–1107.
23. Cherkasov A, Hilpert K, Jenssen H, Fjell CD, Waldbrook M, Mullaly SC, Volkmer R and Hancock RE. Use of artificial intelligence in the design of small peptide antibiotics effective against a broad spectrum of highly antibiotic-resistant superbugs. ACS Chem Biol 2009;4:65–74.
24. Hilpert K, Volkmer-Engert R, Walter T, Hancock REW. High-throughput generation of small antibacterial peptides with improved activity. Nat Biotechnol 2005;23:1008–1012.
25. Moskowitz JS, Blaisse MR, Samuel RE, Hsu H, Harris MB, Martin SD, Lee JC, Spector M, Hammond PT. The effectiveness of the controlled release of gentamicin from polyelectrolyte multilayers in the treatment of *Staphylococcus aureus* infection in a rabbit bone model. Biomaterials 2010;31:6019–6030.
26. Popat KC, Eltgroth M, LaTempa TJ, Grimes CA, Desai TA. Decreased *Staphylococcus epidermis* adhesion and increased osteoblast functionality on antibiotic-loaded titania nanotubes. Biomaterials 2007;28:4880–4888.
27. Macak JM, Tsuchiya H, Ghicov A, Yasuda K, Hahn R, Bauer S, Schmuki P. $TiO_2$ nanotubes: self-organized electrochemical formation, properties and applications. Curr Opin Solid State Mater Sci 2007;11:3–18.
28. Kim SE, Lim JH, Lee SC, Nam S, Kang H, Choi J. Anodically nanostructured titanium oxides for implant applications. Electrochim Acta 2008;53:4846–4851.
29. Losic D, Simovic S. Self-ordered nanopore and nanotube platforms for drug delivery applications. Expert Opin Drug Deliv 2009;6:1363–1381.
30. Balaur E, Macak JM, Taveira L, Schmuki P. Tailoring the wettability of $TiO_2$ nanotube layers. Electrochem Commun 2005;7:1066–1070.
31. Vasilev K, Poh Z, Kant K, Chan J, Michelmore A, Losic D. Tailoring the surface functionalities of titania nanotube arrays. Biomaterials 2010;31:532–540.
32. Wang D, Liu Y, Liu X, Zhou F, Liu W, Xue Q. Towards a tunable and switchable water adhesion on a $TiO_2$ nanotube film with patterned wettability. Chem Commun 2009:7018–7020.
33. Oh S, Daraio C, Chen LH, Pisanic TR, Finones RR, Jin S. Significantly accelerated osteoblast cell growth on aligned TiO2 nanotubes. J Biomed Mater Res A 2006;78:97–103.

34. Bjursten LM, Rasmusson L, Oh S, Smith GC, Brammer KS, Jin S. Titanium dioxide nanotubes enhance bone bonding in vivo. J Biomed Mater Res A 2010;92:1218–1224.

35. Brammer KS, Oh S, Cobb CJ, Bjursten LM, Van der Heyde H, Jin S. Improved bone-forming functionality on diameter-controlled TiO2 nanotube surface. Acta Biomater 2009;5:3215–3223.

36. Von Wilmowsky C, Bauer S, Lutz R, Meisel M, Neukam FW, Toyoshima T, et al. In vivo evaluation of anodic $TiO_2$ nanotubes: An experimental study in the pig. J Biomed Mater Res B Appl Biomater 2009;89:165–171.

37. Peng L, Mendelsohn AD, LaTempa TJ, Yoriya S, Grimes CA, Desai TA. Long-term small molecule and protein elution from $TiO_2$ nanotubes. Nano Lett 2009;9:1932–1936.

38. Popat KC, Eltgroth M, La Tempa TJ, Grimes CA, Desai TA. Titania nanotubes: A novel platform for drug-eluting coatings for medical implants? Small 2007;3:1878–1881.

39. Macak JM, Albu SP, Schmuki P. Towards ideal hexagonal self-ordering of $TiO_2$ nanotubes. Phys Status Solidi-Rapid Res Lett 2007;1:181–183.

40. Li S, Zhang G, Guo D, Yu L, Zhang W. Anodization fabrication of highly ordered $TiO_2$ nanotubes. J Phys Chem C 2009;113: 12759–12765.

41. Macak JM, Schmuki P. Anodic growth of self-organized anodic $TiO_2$ nanotubes in viscous electrolytes. Electrochim Acta 2006;52: 1258–1264.

42. Regonini D, Jaroenworaluck A, Stevens R, Bowen CR. Effect of heat treatment on the properties and structure of $TiO_2$ nanotubes: Phase composition and chemical composition. Surf Interface Anal 2010;42:139–144.

43. Regonini D. Anodised $TiO_2$ Nanotubes: Synthesis, Growth Mechanism and Thermal Stability. PhD Thesis. University of Bath: Bath, UK; 2008.

44. Hilpert K, Elliott M, Jenssen H, Kindrachuk J, Fjell CD, Koerner J, Winkler DFH, Weaver LL, Henklein P, Ulrich AS, Chiang SHY, Farmer SW, Pante N, Volkmer R, Hancock REW. Screening and characterization of surface-tethered cationic peptides for antimicrobial activity. Chem Biol 2009;16:58–69.

45. Zwilling V, Darque-Ceretti E, Boutry-Forveille A, David D, Perrin MY, Aucouturier M. Structure and physicochemistry of anodic oxide films on titanium and TA6V alloy. Surf Interface Anal 1999; 27:629–637.

46. Prakasam HE, Shankar K, Paulose M, Varghese OK, Grimes CA. A new benchmark for $TiO_2$ nanotube array growth by anodization. J Phys Chem C 2007;111:7235–7241.

47. Hetrick EM, Schoenfisch MH. Reducing implant-related infections: Active release strategies. Chem Soc Rev 2006;35:780–789.

48. Wu P, Grainger DW. Drug/device combinations for local drug therapies and infection prophylaxis. Biomaterials 2006;27: 2450–2467.

49. Ellingsen JE. A study on the mechanism of protein adsorption to $TiO_2$. Biomaterials 1991;12:593–596.

50. Sousa SR, Moradas-Ferreira P, Saramago B, Melo LV, Barbosa MA. Human serum albumin adsorption on $TiO_2$ from single protein solutions and from plasma. Langmuir 2004;20:9745–9754.

51. Cacciafesta P, Humphris ADL, Jandt KD, Miles MJ. Human plasma fibrinogen adsorption on ultraflat titanium oxide surfaces studied with atomic force microscopy. Langmuir 2000;16:8167–8175.

52. Topoglidis E, Cass AEG, Gilardi G, Sadeghi S, Beaumont N, Durrant JR. Protein adsorption on nanocrystalline $TiO_2$ films: An immobilization strategy for bioanalytical devices. Anal Chem 1998;70:5111–5113.

53. Liang H, Li X, Yang Y, Sze K. Effects of dissolved oxygen, pH, and anions on the 2,3-dichlorophenol degradation by photocatalytic reaction with anodic $TiO_2$ nanotube films. Chemosphere 2008;73: 805–812.

54. Wang N, Lin H, Li JB, Yang XZ, Chi B. Electrophoretic deposition and optical property of titania nanotubes films. Thin Solid Films 2006;496:649–652.

55. Tsuchiya H, Macak JM, Muller L, Kunze J, Muller F, Greil P, Virtanen S, Schmuki P. Hydroxyapatite growth on anodic $TiO_2$ nanotubes. J Biomed Mater Res A 2006;77:534–541.

56. Uchida M, Kim HM, Kokubo T, Fujibayashi S, Nakamura T. Structural dependence of apatite formation on titania gels in a simulated body fluid. J Biomed Mater Res A 2003;64:164–170.

57. Yu W, Qiu J, Xu L, Zhang F. Corrosion behaviors of $TiO_2$ nanotube layers on titanium in Hank's solution. Biomed Mater 2009;4: 065012.